

# Operation and Performance of Wind Generators in Tappi wind Park

Tomoyuki MATSUZAKA\*, Keiichi TUCHIYA\*\*, Sayoshi YAMADA\*\*

## Abstract

Tohoku Electric Power Company has made investigations on natural energy resources such as wind energy, tidal energy and solar energy so far. On the basis of the research, we built Tappi wind park at March, 1992. The wind park is the biggest one in Japan. This paper presents the wind climate of the site, machine specifications, generator system and generated power.

## 1. WIND CLIMATE OF TAPPI

Tappi is located at the tip of Tsugaru peninsula of the main island of Japan. Figure 1 shows wind speed distribution. The average wind speed is about 10 m/s at 20 m height above ground level, and frequent components of wind direction are E, WNW and SW. The wind climate is one of the most promising sites of Japan.

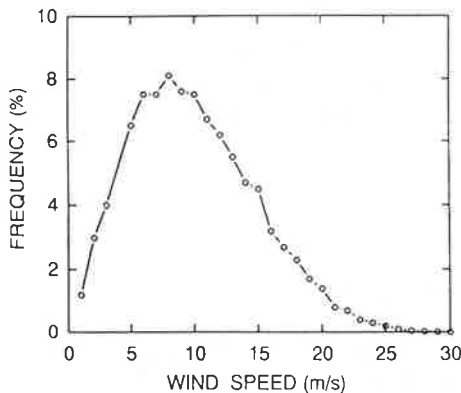


Fig. 1. Wind Speed Distribution

## 2. MACHINE SPECIFICATIONS

The wind park consists of five wind generators with a total power of 1.375 Kw. Each generator is a 275 Kw induction machine of same unit. In near future, more five units are planned to be installed. The machine specifications are the following.

### *Rotor*

Type	Horizontal
Rotational speed	43 rpm
Hub height	30 m
Diameter	28 m
Number of blades	3
Cut-in speed	5 m/s
Cut-out speed	24 m/s
Material	GFRP

### *Generator*

Type	Induction
Voltage	440 V
Rotational speed	1,500 rpm

## 3. GENERATOR SYSTEM

A wind generator consists of a wind turbine, an induction generator, power system and control system.

平成 5 年 12 月 15 日受理

\* Hachinohe Institute of Technology

\*\* Tohoku Electric Power Company

### Wind Turbine

Figure 2 shows wind turbine characteristics. The pitch angle is fixed at  $-90$  deg. below  $5$  m/s of wind speed, and at  $-10$  deg. from  $5$  m/s to  $13$  m/s of wind speed, and is controlled in the region of  $-10 \sim -35$  deg. depending on wind speed, and is set to  $-90$  deg. to cut-out over  $24$  m/s of wind speed. The dynamical equations are described as

$$sJ\Omega = T_w - T_g \quad (1)$$

$$T_w = C_t(\rho\pi R^3/2)V^2 \quad (2)$$

$C_t$  is approximated as the following function over operational range.

$$C_t = -(c_1\beta^2 + c_2)\lambda + c_3/(c_4 + \beta^2) \quad (3)$$

### Induction Generator

The cage rotor induction generators are used as generators. The machine model is described by  $d$ - $q$  axis equation.

$$\left. \begin{aligned} v_{1d} &= (R_1 + sL_1)i_{1d} + sMi_{2d} \\ v_{1q} &= (R_1 + sL_1)i_{1q} + sMi_{2q} \\ 0 &= sMi_{1d} + \omega Mi_{1q} + (R_2 + sL_2)i_{2d} + \omega L_2 i_{2q} \\ 0 &= -\omega Mi_{1d} + sMi_{1q} - \omega L_2 i_{2d} + (R_2 - sL_2)i_{2q} \end{aligned} \right\} \quad (4)$$

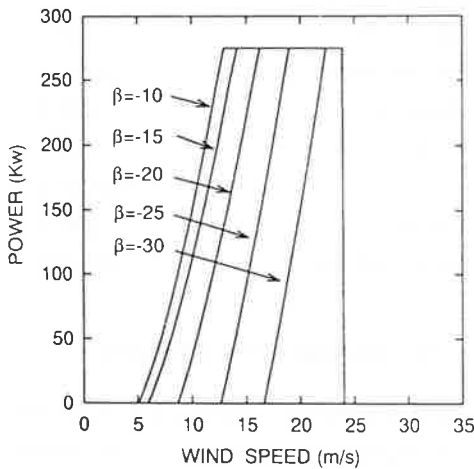


Fig. 2. Generator Characteristics

$$\left. \begin{aligned} T_g &= M(i_{1q}i_{2d} - i_{1d}i_{2q}) \\ P_g &= \omega T_g \end{aligned} \right\} \quad (5)$$

### Power System

Figure 3 shows power system to be connected with the generator. This model is used to evaluate voltage variation at injection node of power system due to rush current at grid connection. The voltage change at the node is described as

$$\Delta V_g = -\left(R'_1 i_g + L'_1 \frac{di_g}{dt}\right) \quad (6)$$

where

$$i_g = \sqrt{\frac{2}{3}} i_{1d} \quad (7)$$

### Controller

Figure 4 shows the blockdiagram of con-

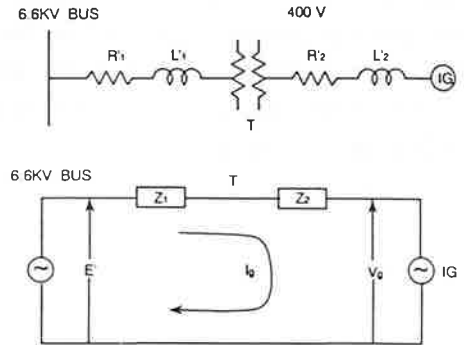


Fig. 3. Power System

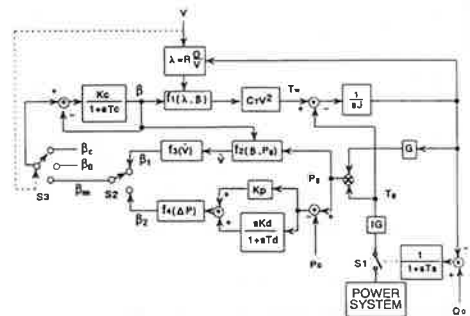


Fig. 4. Blockdiagram of Control System

troller. Torque coefficient  $C_t$  is obtained as a function of tip speed ratio  $\lambda$  and pitch angle  $\beta$ , and then  $T_w$  is computed from equations (2) and (3). The generator power  $P_g$  is obtained from a product of  $T_g$  which is given by equation (5), and  $\Omega_{GP}(=\omega)$ . The estimated wind speed  $\hat{V}$  is given as the output of function  $f_2(\beta, P_g)$ .  $\hat{V}$  is used instead of raw wind speed in arithmetic operation of controller since it is smoothed with rotor inertia of wind turbine and free from noises.  $\beta_1$  is given as the output of function  $f_3(\hat{V})$ , and gives static operating point of pitch angle. Furthermore,  $\Delta P = P_g - P_0$  is impressed to  $PD$  controller, and its output is provided to function  $f_4(\Delta P)$ .  $\beta_2$  is the output of function  $f_4(\Delta P)$ , and gives dynamic pitch angle. The switch  $S_2$  selects the maximum value of  $\beta_1$  and  $\beta_2$ .  $\beta_c$  is cut-out pitch angle, and  $\beta_0$  is the fixed pitch angle between 5 m/s and 13 m/s of wind speed, and  $\beta_m$  is varied depending on wind speed between 13 m/s and 24 m/s.  $S_3$  selects these conditions depending on wind speed, and controls pitch angle with the pitch controller.  $S_1$  is the switch to interconnect the induction generator to power system.

#### 4. OPERATIONAL CHARACTERISTICS

Here we clarify the over all characteristics through simulation using models above mentioned and then make comparison between simulation results and measurements. We make two case simulations: a) transient state and b) quasi transient state. First case is the state when the wind machine is switched to power system, where time constants of electrical system are dominant and those of mechanical system are ineffective. This study is necessary to evalu-

ate voltage variation at generator interconnection node to power system. As is generally known, induction generators cause voltage variation when interconnected into grid. Utility company has an obligation to keep the variation within allowable value, and hence it is important to evaluate voltage regulation. Second case is the state where the transient state elapsed and the system is under normal operation, where time constants of electrical system are ineffective and this is necessary to evaluate system parameters of control system and functions.

Figure 5 and Figure 6 depict comparison between measurements and simulation in first case and in second case respectively. From Figure 5, we can admit close agreement between measurement and simulation. In Figure 6, we can recognize some deviation in detail points. One reason seems to be due to our assumption that the wind turbine is always facing to wind direction while the actual yaw control does not follow it. The other reason may be due to inaccurate system parameters.

#### 5. GENERATED POWER, AVAILABILITY AND CAPACITY FACTOR

In this section, we describe generated power in Tappi wind park. The wind generators are under operation interconnected with grid since April, 1992. Figure 7 shows generated power (MWh) during this period. Total generated power was 2,229 MWh. This is less power than we had estimated. One reason is that the average wind speed adopted in planning was stronger than the value we observed in 1992. The other reason is that we had to stop the machines for several tests and maintenance. Figure 8 is

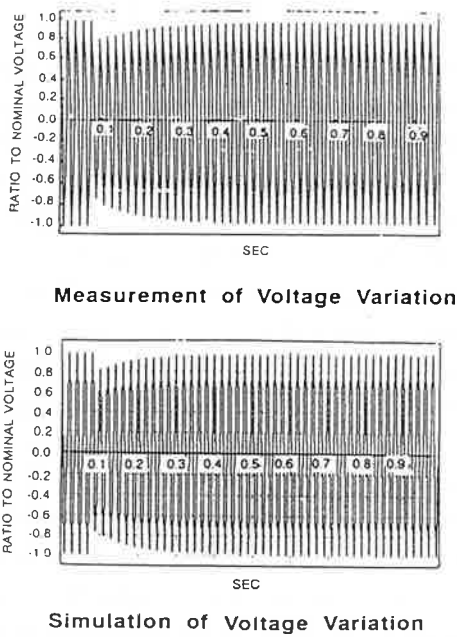


Fig. 5. Comparison between Measurement and Simulation of Voltage Variation

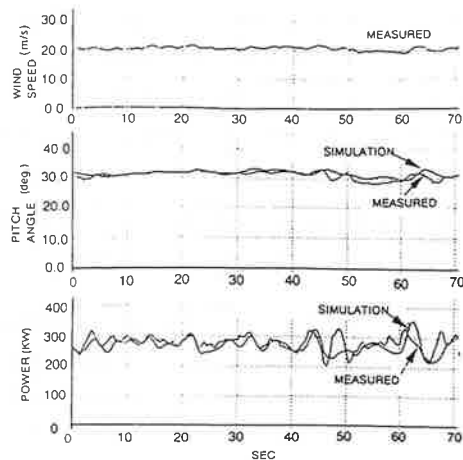


Fig. 6. Comparison between Measurement and Simulation of Pitch Angle and Power

availability of each machine, and the average availability is 47.6% during 20,842 hours of total operation time of all machines. Figure 9 shows capacity factor. The average value is 19.1% through one year.

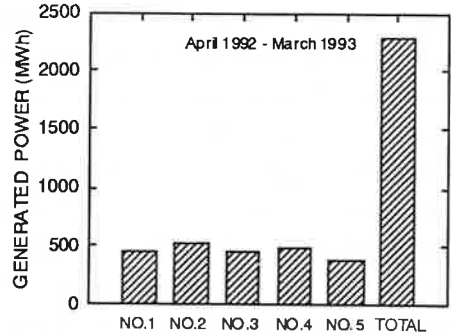


Fig. 7. Generated power

## 6. NOISE

We studied attenuation characteristics of noise level versus distance using one generator. As the result we found that the noise

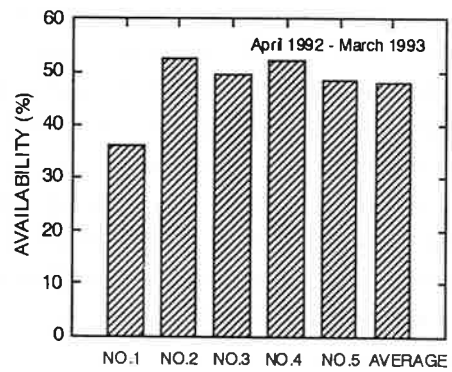


Fig. 8. Availability

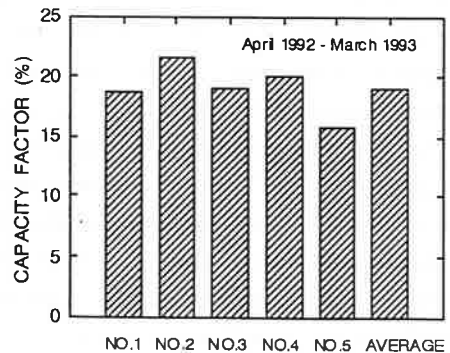


Fig. 9. Capacity factor

level decayed following the well known rule  $-6\text{dB}$  attenuation per square of distance. Figure 10 shows noise attenuation characteristics. From the Figure, we are able to estimate about 46 dB at a house two hundred meter far away from the nearest turbine. This noise level seems to be negligible. Figure 11 shows frequency spectrum. The noise from the gear box proved to be most significant by investigations.

## 7. ICING

We have not observed icing to blades during operation so far. However, the test period is too short to make conclusion. So, we are continuing further observation.

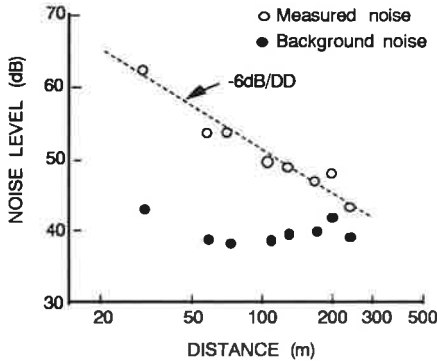


Fig. 10. Noise vs. distance

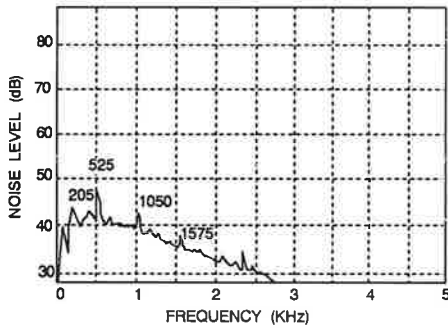


Fig. 11. Noise spectrum

## 8. CONCLUSION

First, we described wind climate of Tappi wind park, machine specifications. Second, we presented a generator model to study voltage regulation at grid interconnection and controller operation. We evaluated the model validity through measurements and simulations, and confirmed that simulation results agreed approximately with measurements. Third, we stated operational characteristics such as generated power, availability, capacity factor. Finally, we described noise problem and icing. However, we need more observations to evaluate over all performance correctly.

## ACKNOWLEDGMENTS

We would like to express our thanks to those of Mitsubishi Heavy Industry Co., Ltd. who gave corporation to this study.

## NOMENCLATURE

- $J$  : moment of inertia
- $R$  : radius
- $G$  : gear ratio
- $\lambda$  : tip speed ratio
- $\beta$  : pitch angle
- $C_t$  : torque coefficient  $= f_1(\lambda, \beta)$
- $s = \frac{d}{dt}$
- $\Omega$  : angular speed
- $\Omega_0$  : rated angular speed
- $V$  : wind speed
- $\hat{V}$  : estimated wind speed
- $T_w$  : aerodynamic torque
- $K_t = \rho \pi R^3 / 2$
- $\rho$  : air density

$R_1, R_2$ : resistance of power line  
 $L_1, L_2$ : inductance of power line  
 $Z_1, Z_2$ : impedance of power line  
 $V_g$ : generator voltage  
 $I_g$ : generator current  
 $K_c, T_c$ : pitch controller constants  
 $K_p, K_d, T_d$ : PD controller constants  
 $\hat{V} = f_2(\beta, P_g)$   
 $\beta_1 = f_3(\hat{V})$   
 $\beta_2 = f_4(\Delta P)$   
 $\beta_m = \text{Max}(\beta_1, \beta_2)$   
 $IG$ : induction generator  
 $T_s$ : time constant of switch  
 $P_g$ : generator power  
 $P_0$ : reference power  
 $T_g$ : electrical torque

## REFERENCES

- (1) T. Matsuzaka, K. Tuchiya, S. Yamada, Operation and performance of wind generators in Tappi wind park, Proceedings of New Energy Systems and Conversions, pp. 579-583, Yokohama, Japan, 1993
- (2) K. Tuchiya, T. Matsuzaka, Simulation of operating characteristics of a wind energy conversion system, pp. 752-759, Trans. IEE of Japan, Vol. 113-B, No. 7, Jan., 1993
- (3) T. Matsuzaka et al., Voltage fluctuation simulation of power system due to a wind driven induction generator, Proceedings of Asian and Pacific area wind energy conference, pp. 124-127, Shanghai, China, 1988
- (4) K. Sasaki, T. Matsuzaka, K. Tuchiya, Voltage Fluctuation Simulation of Power System due to a Wind Driven Induction Generator, pp. 33-39, Trans. IEE of Japan, Vol. 110B, No. 1, Jan., 1990